Quasi real-time post-earthquake damage assessment of lifeline systems based on available intensity measure maps

Marco Torbol[*]

School of Urban and Environmental Engineering, Ulsan National Institute of Science and Technology
50 UNIST-gil, Eonyang-eup, Ulju-gun, Ulsan 689-798, Republic of Korea

Abstract. In civil engineering, probabilistic seismic risk assessment is used to predict the economic damage to a lifeline system of possible future earthquakes. The results are used to plan mitigation measures and to strengthen the structures where necessary. Instead, after an earthquake public authorities need mathematical models that compute: the damage caused by the earthquake to the individual vulnerable components and links, and the global behavior of the lifeline system. In this study, a framework that was developed and used for prediction purpose is modified to assess the consequences of an earthquake in quasi real-time after such earthquake happened. This is possible because nowadays entire seismic regions are instrumented with tight networks of strong motion stations, which provide and broadcast accurate intensity measure maps of the event to the public within minutes. The framework uses the broadcasted map and calculates the damage to the lifeline system and its component in quasi real-time. The results give the authorities the most likely status of the system. This helps emergency personnel to deal with the damage and to prioritize visual inspections and repairs. A highway transportation network is used as a test bed but any lifeline system can be analyzed.

Keywords: seismic risk; safety & reliability; lifeline systems; distributed systems

1. Introduction

After an earthquake public authorities need information about the damage sustained by the lifeline systems. However, up to 1994 Northridge earthquake in California and 1995 Kobe earthquake in Japan, the only information available was the earthquake epicenter and magnitude. These two numbers are not enough to prioritize visual inspections or to provide useful information to emergency personnel because they do not contain any data on the intensity measure of the earthquake over the region of interest. As stated by (Yamakawa 1998) Japanese government failed to immediately recognize the size of the damage caused by Kobe earthquake. After these two major events efforts were made to improve the state of the art for earthquake detection systems, propagation models, and to include real time broadcasting technology. New intensity measure maps that represent earthquakes were developed and made available, such as: Shake map in US (Fig. 1(a)) and JMA instrumental intensity map in Japan (Fig. 1(b)).

In US, Shake map was proposed by (Wald *et al*. 1996) and developed over the years by (Wald

---

*Corresponding author, Assistant Professor, E-mail: mtorbol@unist.ac.kr

et al. 1999a) (Wald *et al*. 1999b) (Wald *et al.* 2006). Shake maps are generated using field data, empirical attenuation relationships and correlation functions between nearby strong motion stations. The field data are retrieved from a tight network of stations equipped with tri-axial accelerometer sensors. The empirical attenuation relationships are developed based on past events and regression analysis. The correlation functions are used to reduce the uncertainty of the prediction and to mitigate the effect of outlier. The correlation between the intensity measure at the station of interest and the intensity measure at nearby stations is computed based on past events and used to adjust the values of new events. The result is a map of the region that specifies an intensity measure of the earthquake, such as PGA, PGV, $S_a(0.3s)$, $S_a(1.0s)$, $S_a(3.0s)$ on a grid.

Nowadays, after an earthquake intensity measure maps are automatically generated and broadcasted. For example, USGS broadcasts the Shake maps of an earthquake within minutes using the ShakeCast broadcasting software (Wald *et al*. 2008). In this study, a framework that takes advantage of this broadcast technology is used to estimate the damage to a lifeline system and its components in quasi real-time, less than a minute using a laptop computer. The damage is expressed by both local indexes, such as the damage to vulnerable components or subsystems, and global indexes, that express the global behavior of the lifeline system. The framework developed to perform the simulations and to compute global and local indexes is based on (Torbol and Shinozuka 2014). The original framework was developed for the Probabilistic Seismic Risk Assessment (PSRA) of highway transportation networks. However, it was improved to accept Shake maps and other intensity measure maps as the earthquake scenario input and it can work along with ShakeCast to perform quasi real-time post-earthquake damage assessment. ShakeCast is used to distribute a Shake map to the recipients connected to the system. A recipient uses the map to assess the damage to the dataset of structures under his supervision. For example, (Fraser *et al*. 2008) used the broadcasted maps to perform the post-earthquake damage assessment of the dams under their supervision. Instead, this study uses the broadcasted maps not only to assess the damage to the single components of the network but also to estimate the overall impact on the entire highway network. How extensive is the damage of this earthquake? What level of network disruption can be expected? How much damage to the economy of the region was caused?

The framework was tested on the Los Angeles – Orange County highway transportation network. Bridges are the vulnerable components. Highways are the links between the network nodes. Drivers' delay is used to represent the global damage index of the network. The results show how the framework can simulate the damage to the network and compute the different damage indexes. They also show how the damage is not only a function of the magnitude of the earthquake but also a function of the network topology and spatial distribution. The framework is not limited to highway transportation network but it can be used for other lifeline systems, such as: power grids or water distribution systems.

2. Methodology

The methodology is illustrated in Fig. 2. First, the properties of the lifeline system are collected including: the fragility curves of the vulnerable components, the spatial distribution of links and nodes, and the load on the system. Second, the intensity measure map is received by the broadcasting agency minutes after the earthquake. Third, Monte Carlo simulation is used to compute the average damage to the vulnerable components, its uncertainty, and the global impact on the network. The results include: local damage indexes, such as the average damage to the links

and the bridges, and global damage indexes, such as social loss, which is a function of the global behavior of the network.

An intensity measure map defines one single earthquake scenario. In this study, the hazard is not probabilistic but it is one well defined event. In this context, hazard curves and hazard maps are not important and not considered. However, within each single event the uncertainty on the vulnerability of the components is taken into consideration. A comparison can be made between this study and the previous study by (Torbol and Shinozuka 2014). The previous study uses a data set of earthquake scenario, which matches the hazard of the region, as hazard input. PSRA of the highway transportation network is performed and the results are expressed in term of a seismic risk curve, which represents the social loss over a time period $/day as a function of the yearly probability of occurrence λ_y. Instead, this study uses a single intensity measure map, which represents a unique event, the event happens now and the probability of occurrence is 1. The damage assessment over the network is performed for the event. Because the damage assessment is for a single event special attention is given to output parameters, such as status of the vulnerable components and status of the links including their uncertainty. These outputs are important to understand the damage within the system.
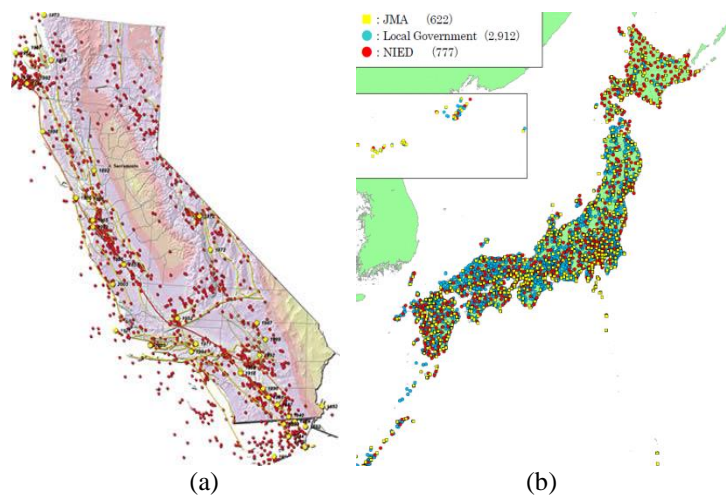

Fig. 1 Network of strong motion stations: (a) California and (b) Japan
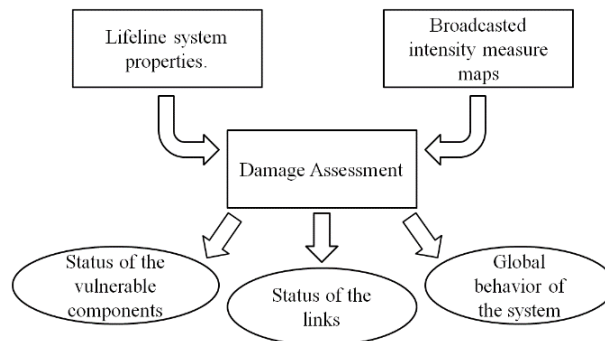
Fig. 2 Post-earthquake risk assessment flow-chart

3. Intensity measure maps

As stated in the introduction, before 1994 Northridge earthquake and 1995 Kobe earthquake the only available information after an earthquake were its magnitude and its epicenter. This is not enough to estimate the shaking intensity of the earthquake over a large area. Spatial variation of the characteristics of the basin and local soil conditions affects the way a seismic wave propagates. For example, in 1971 San Fernando earthquake the highest level of shaking was close to the epicenter. Instead, during 1989 Loma Pietra and 1994 Northridge earthquake high level of shaking were also felt far away. Areas were the seismic wave was amplified by the local soil conditions or other properties of the basin.

In United States, after 1994 Northridge earthquake a lot of efforts and economic resources were made available by United States Geological Survey (USGS), Federal Emergency Management Agency (FEMA), National Science Foundation (NSF), and many other agencies to develop a new tool capable of representing an earthquake over the entire affected region. Shake maps are the result of these efforts. They represent the earthquake with an intensities measure map of the region. They are the current usable state of the art and are available in term of Instrumental Intensity (Fig. 3(a)), Peak Ground Acceleration (PGA) (Fig. 3(b)), Peak Ground Velocity (PGV) (Fig. 3(c)), and Spectral Acceleration (S_a) at 0.3, 1.0, 3.0 sec (Fig. 3(d)). However, the Instrumental Intensity is not a strong motion parameter but it is useful to the public to understand the intensity of the earthquake. Countries like Japan and Taiwan developed their own intensity measure maps. In the future, rather than a simple intensity measure the wave form of the seismic wave will be available at any point of a region. Nowadays, this research is currently on going. For example, (Olsen *et al*. 2008) developed software that model the seismic wave from the fault rupture over the entire basin. However, this software requires hours of supercomputing time.

This study uses the broadcasted intensity measure maps to assess the status of the lifeline system. After each earthquake the national agency automatically generates and broadcasts the intensity measure maps to the public. For example, USGS uses Rich Site Summary (RSS feed) technology to broadcast Shake maps in quasi-real time after every earthquake. Every time an intensity measure map is available the framework performs the damage assessment of the lifeline system under consideration.

A Shake map is generated based on: the field data, an empirical attenuation relationship, and correlation functions. The field data are retrieved from a network of strong-motion stations. However, it is not feasible to send the entire time history in real time to the base station due to the large amount of data gathered, bandwidth limitations, and connection type. For example, some stations are still working with dial-up connection. Therefore, the strong motion parameters are computed by each station and sent to the base.

Shake map describes one of the intensity measures of the earthquake using a grid of points that is more refined than the network of strong-motion stations. Therefore, while many points are directly associated with a strong-motion station many other are not, especially in rural areas. Phantom stations are used in this case. The intensity measure at a phantom station is calculated in three steps. First, an empirical attenuation relationship is used to calculate the intensity measure based on: the magnitude of the earthquake, the epicenter distance and the local soil conditions. Second, a bias correction is applied to this initial value. The bias-factor uses field data at nearby stations, where the difference between the recorded value and the empirical value is computed. Nearby stations are defined as the stations in 120 km radius from the phantom station (Fig. 4). Finally, the bias factor has a lower and upper bound. Therefore, the corrected value will be within

a certain range of the initially calculated empirical value.

Phantom stations are not limited to grid points not associated with a real station but they are also used if a real station do not deliver its data within a certain time period or the data seem an outlier, as stated by (Wald *et al*. 1996). Furthermore, a Shake map is updated many times after an earthquake for different reasons, such as: corrections to the initial magnitude estimation of the earthquake, which is used in the empirical attenuation relationship, new data from the stations are available or new information about the rupture mechanism.

In US, intensity measure maps are available from two different sources. The first source is the USGS database, which contains Shake maps of past-event and hypothetical future scenarios. The second source is ShakeCast, which is a framework to broadcast newly generated Shake map within minutes of an earthquake. With ShakeCast providing quasi-real time maps the users have to and are free to develop their own framework to perform damage assessment of their property. ShakeCast is used by many agencies in California, such as: California transportation department (Caltrans), and Los Angeles Unified School District (LAUSD). Shake map and ShakeCast were used by (Fraser *et al*. 2008) to establish a post-earthquake damage inspection of the 1,200 dams of the Division of Safety of Dams (DSOD) in California.
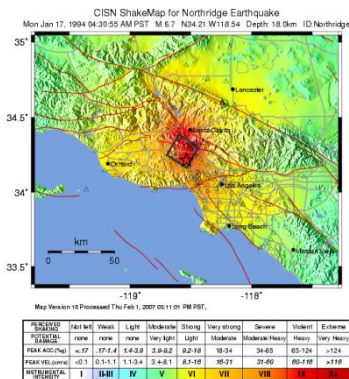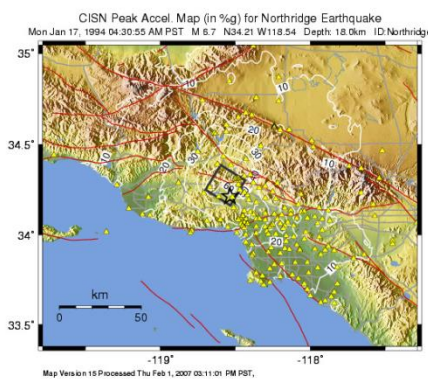
(a) Instrumental Intensity   (b) PGA
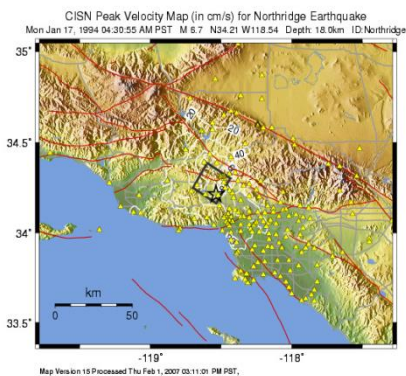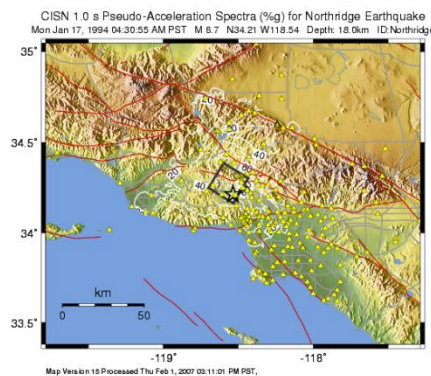
(c) PGV   (d) S_a(1.0s)

Fig. 3 Shake maps of Northridge earthquake
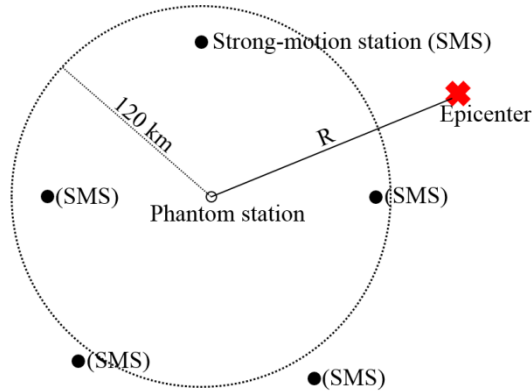
Fig. 4 Phantom station correlation distance

Different national agencies around the world operate their own network of sensors and produces their own intensity measure maps. In Japan, the Japan Meteorological Agency (JMA) operates two major networks. The K-NET network, which is composed by free field strong-motion stations placed all over Japan on the surface, such as municipality and school yards. The KiK-net network, which is composed by strong-motion stations placed in borehole up to 3,000 m deep. Together these networks have more than 2,000 stations throughout Japan. Another similar network with over 600 stations is operated by Tokyo gas. This network automatically shut off gas distribution when the ground motion exceeds a predetermined threshold (Yamazaki *et al.* 1995). In Taiwan, the Central Weather Bureau operates a network of free-field strong-motion stations, more than 600. This network is used for the earthquake Rapid-Reporting System (RSS) and the Earthquake Early Warning (EEW) system (Shin *et al.* 2002).

In this study USGS's Shake maps are used as inputs but any intensity measure maps can be used as long as the probability of failure of the vulnerable components are expressed as a function of the same intensity measure. For example, Japan maps are given in term of JMA Instrumental Intensity. The JMA Instrumental Intensity is computed at each recording station with a two steps process: a band pass filter in the frequency domain and the durational effect of PGA, which is the sum of all intervals Δt where the acceleration exceeds a reference PGA JMA (1996). Before using these maps the JMA Instrumental Intensity must be converted to a strong motion parameter, such as PGA, PGV, or SI. For example, the conversion can be performed based on the formulas given by (Karim and Yamazaki 2002), Eq. (1)-(3).

$$I_{JMA} = -0.65 + 0.18M + 1.81\log_{10} PGA_R \tag{1}$$

$$I_{JMA} = 3.35 - 0.13M + 1.82\log_{10} PGV_R \tag{2}$$

$$I_{JMA} = 2.61 - 0.03M + 1.92\log_{10} SI_R \tag{3}$$

JMA Instrumental Intensity was converted to PGA while testing the framework for a highway network in Japan.

4. Damage assessment of lifeline systems

The seismic risk assessment of lifeline systems can be divided in two categories based on its purpose. PSRA is performed during normal operational conditions. The earthquake hazard is treated probabilistically using inputs from Probabilistic Seismic Hazard Analysis (PSHA). The computed seismic risk is expressed in term of social loss vs. probability of occurrence. The social loss expresses the consequences on the society that the disruption of the lifeline system causes due to the earthquake. Different lifeline systems require different global damage indexes to describe the disruption but social loss can always be reduced to "$/day lost" due to the earthquake. Damage assessment is performed in post-earthquake conditions. The different authorities are interested in the actual damage that the event causes. Information about the actual damage is usually collected through visual inspections. However, if the properties of the system and the intensity measure map of the earthquake are known the damage can be simulated immediately. The results represent the actual damage with a certain degree of uncertainty. However, they can be used to prioritize the visual inspections and to help emergency personnel that deal with the system. If the lifeline system is a highway transportation network the result can be used to navigate the network avoiding the most damaged links.

Given the intensity measure map of the earthquake and the properties of the system, it is possible to calculate: the probability density function of the social loss caused by the earthquake, the probability of each vulnerable components being in any damage state, which can also be derived directly from the fragility curves, and the probability of each link being in any damage state. It is possible to rank the vulnerable components and the links in accordance to their impact on the overall performance of the network. In the simulation presented the existing framework for PSRA of highway network was extended to compute these parameters in post-earthquake conditions.

4.1 Probabilistic seismic risk assessment

During normal operational conditions public authorities, insurance companies, building owners, and real estate companies perform PSRA of civil structures and infrastructures, such as: individual building, residential area, commercial areas, bridges, and power distribution grids, water distribution systems, highway networks. Benefit/cost analyses are based on these results for different purposes. An insurance company adjusts the insurance rate on it. A transportation authority plans strengthening programs on its bridge inventory. A real estate company adjust the estimation of the value of a property.

For an individual structure, the hazard curve associated with the location of the structure and the fragility curves of the structure are used to calculate the seismic risk curve. The hazard curve expresses the probability of occurrence of an earthquake versus one of its intensity measure, usually PGA, PGV, or $S_a(\omega_{n,1})$. The hazard curve can be retrieved from the national agency with competence on earthquake, such as USGS, JMA, CWB. The fragility curves express the probability of exceeding a damage state versus the intensity measure of the earthquake. A fragility curve is obtained either empirically from past events or analytically from computer simulation.

For lifeline systems, analytical and empirical fragility curves can be used to represent the vulnerable components of the system, such as substation, switches, and power-lines for power distribution grids or bridges for highway transportation networks. However, an earthquake scenario is necessary to represent the earthquake. Furthermore a data set of earthquake scenarios is

necessary because the hazard input must be in agreement with the hazard curve at any location in the region, i.e., it has to agree with the hazard maps for any probability of occurrence.

4.2 Post-earthquake damage assessment

In PSRA of lifeline systems the result of interest is the social loss caused by the disruption of the network. In post-earthquake damage assessment the results of interest are: the performance of the network, the damage to specific links, and the damage to specific vulnerable components. The damage to the links is useful to decide flow rerouting and the damage to the components is useful to prioritize visual inspections and to organize emergency repairs. Fragility curves are used to represent the damageability of the vulnerable components but fragility curves express the probability of exceeding a given damage state as a function of the intensity measure of the earthquake. Therefore, Monte Carlo simulations have to be used to generate a certain number of possible damaged systems. Each damaged system is a possible outcome. In the *ith* simulation a random number is taken on each vulnerable component and it is compared with the probability of exceeding each damage state. The outcome of this comparison decides the status of the vulnerable component for the *ith* simulation.

In this study, a highway transportation network was used as test bed. The fragility curves of the bridges are taken from (Torbol and Shinozuka 2012), which are analytical fragility curves based on computer simulation. Alternatively, it is possible to use empirical fragility curves, such as: (Shinozuka *et al.* 2000) (Basoz *et al.* 1999), which are based on 1994 Northridge earthquake data, or (Yamazaki *et al.* 1999), which are based on 1995 Kobe earthquake data.

The damage status of the bridges is computed from the outcomes of the Monte Carlo simulations. If infinite numbers of Monte Carlo simulation are performed the probability of a bridge being in any damage state should be equal to the probability from the fragility curves. However, because the number of Monte Carlo simulations is finite the ratio between the fragility curves probability and the simulated probability can be used to quantify how close the results are to the exact solution. The bridges' damage status can be used to prioritize visual inspections and emergency repairs.

The status of each link is based on the status of the vulnerable components inside the link. The damage status of the links is the most useful result because it defines the residual capacity of the links. The residual capacity of the links affects the travel speed and the travel time on the links. These are useful to plan the safest and fastest route to go from point A to point B. For example, to decide the closest hospital or the closest fire fighter station considering not only distance but also damage along the way.

The social loss due to the disruption in the highway transportation network can be represented by the drivers' delay. The links of a damaged network have a reduced traffic flow capacity because of the damage to its bridges. Drivers spend more time within the network to reach their destination. The drivers' delay is the difference between the total travel time of all drivers within the damaged network and the total travel time of all drivers within the intact network, Eq. (4) (Shinozuka *et al.* 2003).

$$DD_{ES_n} = \frac{\sum_{i=1}^{m} \left(TTT_{DN_i} - TTT_{IN} \right)}{m}` \tag{4}$$

where TTT$_{DNi}$ is the total travel time of the *ith* damaged network, TTT$_{IN}$ is the total travel time of the intact network, and m is the number of Monte Carlo simulation.

The total travel time is computed using the user equilibrium analysis, which is a traffic assignment algorithm. The algorithm loads an Origin/Destination matrix (OD matrix), which is based on real field data, on the highway transportation network. The drivers' delay is expressed in hours/day but it can be converted to $/day, which better represent the concept of social loss. In PSRA, drivers' delay versus the reoccurrence rate of the earthquake scenario represents a point of the seismic risk curve. In post-earthquake damage assessment the drivers' delay can be the global index that expresses the amount of disruption caused by the earthquake. It can also be compared with previous earthquake to estimate the severity of the earthquake.

4.2.1 The user equilibrium analysis

The user equilibrium analysis is a mathematical algorithm that guarantee the computation of the lowest possible total travel time of every vehicle over the entire network. Each driver knows that status of the entire network, including the current travel time and flow of each link. Each driver chooses the fastest path to his destination. Because the travel time of a link is based on the current flow on the link the O/D matrix is assigned on the network in k steps. At each step, a 1/k O/D matrix is assigned and the link travel time is updated based on the current flow inside the link. The function used to update the travel time is taken from the Federal Highway Administration, Eq. (5).

$$t_a = t_a^0 \left[1 + \alpha \left(\frac{x_a}{C_a} \right)^{\beta} \right]$$

(5)

where t_a is the travel time of link a at flow x_a; t_a^0 is the travel time of the link a at 0 flow; C_a is the practical capacity of the link; α, β are parameters, $\alpha = 0.15$, $\beta = 0.4$.

The fastest path between two nodes is found by finding the minimum of the following equation

$$z(x) = \sum_a \int_0^{x_a} t_a(\omega) d\omega$$

(6)

where t_a is function of x_a, flow in each link a on the chosen path

$$x_a = \sum_s x_a^s \qquad \forall a$$

(7)

$$\sum_{a \in O_r} x_a^s - \sum_{a \in I_r} x_a^s = q_{rs} \qquad \forall r, s$$

(8)

$$x_a^s \geq 0 \qquad \forall a, s$$

(9)

where x_a^s is the flow of link a on the path s; q_{rs} is the assigned origin-destination flow to be loaded on path s; q_{rs} is a single entry of the input O/D matrix; Or is the set of all inbound links of the

origin node *r* and I_r is the set of all outbound links of the destination node *s*.

The total travel time is

$$TTT = \sum_a x_a t_a \left(x_a \right)$$

(10)

The algorithm was used in previous studies, such as (Shiraki *et al.* 2007). This algorithm compute the smallest total travel time. This allows the computation of the smallest possible drivers' delay. Once the smallest possible drivers' delay is converted to US dollar, the algorithm obtained the smallest benefit. If the smallest benefit is positive the real benefit, which has to be more than this, is also positive.

The drivers' delay time is a representative global damage index because the daily O/D matrix does not vary over a period of few months except if there is a sudden disruption of the network, such as an earthquake. When an earthquake happens the O/D matrix change suddenly but every time a person does not make a trip is a lost business by keeping the same O/D matrix before and after an earthquake the lost business cost is integrated in the drivers' delay (Shinozuka *et al.* 2003)

5. Results

The Los Angeles – Orange County highway transportation network is used as test bed. Previously, this network was used to study the effect of bridge retrofit on network performances (Shinozuka *et al*. 2003) and to study the impact of the directionality effect of ground motion on the PSRA of highway transportation networks (Torbol and Shinozuka 2014). Instead in this study, the network is used as test bed for the quasi real-time post-earthquake damage assessment. The numbers of Monte Carlo simulations necessary to obtain an accurate damage assessment is based on the complexity, spatial distribution, and dimension of the network. 1,000 Monte Carlo simulations for each scenario was set. This number of simulation is necessary to obtain a good accuracy, the mean of the drivers' delay has a confidence interval of less than 3%. If 2 different sets of Monte Carlo simulations of the same scenario are performed their mean values are at most 3% from each other (Torbol and Shinozuka 2014).The average drivers' delay of these simulations represents the social loss caused by the earthquake. Furthermore, the probability distribution function of the number of bridges and the number of links in each damage state is also computed. For each earthquake scenario the comparison of these three indexes gives useful insight about the impact of future possible earthquake on the LA-OC network.

The LA-OC network includes 3,147 bridges of different geometry. These are pre stressed reinforced concrete box girder, single and multiple span. The bridges' decks have multiple level of skew, from 0 to up to 60 deg. The soil condition vary from cat. A, stiff soil, to cat. C, soft soil. The bridges are distributed over 231 links that form the web of the highway network. The links are connected to 148 nodes that represent the highway interchanges inside the network. The computational time for 1,000 Monte Carlo simulation of this network has mean $\mu= 0.421$ sec and standard deviation $\sigma = 0.02$ sec. The simulations were performed in parallel on a 4 cores Intel i5-3230M 2.6 GHz, which is a 2012 CPU for mobile computer. Each core performs the simulations separately. The entire computation for a single scenario takes 106 sec, i.e., less than 2 min. The simulations were also performed on a 4 cores Intel i5-2500 3.3 GHz; each simulation takes 0.163 sec and the entire computation for a single scenario takes less than 40 sec. This is a

reasonable computational time because the LA-OC network is one of the largest highway network worldwide within an urban area.

USGS has 3 different databases of Shake maps: the regular database, the Atlas database, and the earthquake scenario database. The regular database includes Shake map of past earthquakes for each specific region; in this case Southern California. Shake maps are generated based on the data from the network of sensors. The Atlas database includes Shake maps of each past earthquake worldwide. This database is based on data collected worldwide from different networks of sensors. For example, the data in Japan are collected from the Kyonshin network (K-NET), which is independent from USGS. The earthquake scenario database includes synthetic Shake map that are generated through computer simulation based on possible future fault rupture rather than real data. All Shake maps available were used. This includes: 144 Shake map from the earthquake scenario database, 825 Shake map from the regular Southern California database, and 5744 Shake map from the Atlas database. However, an algorithm was included that compares the boundaries of each Shake map with the location of the vulnerable components to determine if the earthquake strikes the system. This automates the process that decides which Shake maps affects the system. Based on this, the seismic risk assessment of the LA-OC highway transportation network was performed for: 31 Shake map of the earthquake scenario database, 267 Shake map from the regular Southern California database, and 66 Shake map from the Atlas database. Tables 1-3 show the results of these analyses. Only Shake maps that caused on average at least one bridge to enter minor damage were reported. The Shake map are ordered based on the level of disruption within the network, i.e., drivers' delay.

As expected, Table 2 show that the worst recorded past earthquake is 1994 Northridge, then 1971 San Fernando, and finally 1987 Whittier Narrows. Other earthquakes, such as 2008 Chino Hill caused a certain amount of damage to the bridges but did not caused any significant disruption to the traffic flow of the highway transportation network. The simulated damage cannot be compared with the real damage because the network that was struck by the earthquake is different from the 2002 network used in the simulation. However, 1994 Northridge earthquake damage (Shinozuka *et al.* 2000) can be compared with the simulated damage.

Table 1 show the results of the Shake map from the earthquake scenario database. The epicenters of 4 earthquake scenarios are shown in Figure 5 and their Shake map in Fig. 6. Interesting is the comparison between the Puente Hills scenario M7.1 (Fig. 6(a)) and the San Joaquin scenario M 6.6 (Fig. 6(b)). While the amount of damage to bridges and links caused by Puente Hills is greater than the damage caused by the San Joaquin the drivers' delays are close. The epicenter of the San Joaquin is placed in the middle of Orange County and it's close to the Pacific coast freeway, I-5 and I-405. This scenario affects every major link that connects Los Angeles to San Diego and it completely disrupts the traffic between these two metropolitan areas. On the contrary, Puente Hills scenario is in the center of Los Angeles, it causes damage to the residential, commercial, industrial area, and infrastructure system but the presence of many major freeways allows efficient rerouting of the traffic and it mitigates the drivers' delay. Another comparison is between Newport Inglewood scenario (Fig. 6(c)) and San Joaquin Hills (Fig. 6(d)). The damage caused to bridges and links is similar but the epicenter of Newport-Inglewood scenario is 15 miles north-east of San Joaquin, which is enough to not affect every major artery simultaneously causing less disruption.

Fig. 7 shows the Probability Density Function (PDF) of each bridge damage states while Fig. 8 show the PDF of the link damage states based on the entire range of Monte Carlo simulations performed for Puente Hills, San Joaquin Hills, Newport Inglewood, and Chino Hills earthquake

scenarios. The parameters of these PDF, mean (μ) and standard deviation (σ), are reported in Table 4 for the bridges and Table 5 for the links.

Table 1 Results of available earthquake scenarios

Earthquake - Scenario database			Network performance [hrs/day]		Bridges status				Link status		
ID	Name	M_w	TTT	Drivers' Delay	min	mod	maj	col	min	mod	maj
53	San Joaquin Hills	6.6	4,496,630	3,573,969	207	150	67	11	34	18	10
60	Puente Hills	7.1	4,350,070	3,427,409	604	408	161	66	91	56	32
71	Chino Hills fault	6.7	2,083,570	1,160,909	104	64	21	3	19	5	1
70	Chino Hills fault	6.7	1,885,680	963,019	104	64	21	3	19	5	1
63	Newport Ingl. fault	6.9	1,723,130	800,469	286	183	64	18	47	22	9
100	Whittier	6.8	1,516,100	593,439	155	95	31	6	27	9	2
114	Northridge (arias sta)	6.7	1,408,070	485,409	129	81	28	11	20	11	5
111	Verdugo fault	6.7	1,366,490	443,829	240	145	46	16	34	17	7
115	Northridge (arias)	6.7	1,167,950	245,289	76	45	14	4	12	5	1
35	V2 scenario aftershock	7.2	1,155,690	233,029	208	126	39	11	32	13	4
113	Northridge	6.7	1,153,680	231,019	94	55	16	5	14	5	1
61	Palos Verdes	7.1	1,135,390	212,729	156	92	27	7	24	9	2
122	Santa Monica fault	6.6	1,130,690	208,029	118	65	17	4	16	5	1
59	Raymond fault	6.5	1,110,640	187,979	177	104	31	11	25	11	4
2	V2 scenario full	7.8	1,060,710	138,049	154	92	29	9	24	8	2
54	SAF southern	7.8	987,261	64,600	101	56	15	4	12	4	1
73	1857 Fort Tejon scenario	7.8	981,532	58,871	105	61	17	6	13	5	2
68	Elsinore fault	6.8	935,917	13,256	10	5	1	0	1	0	0
51	San Jacinto fault (zoom)	6.7	929,903	7,242	26	12	2	0	2	0	0
57	SAF southern	7.4	928,365	5,704	21	10	2	0	2	0	0
55	SAF southern (zoom)	7.4	927,782	5,121	19	9	1	0	1	0	0
62	North Channel	7.4	924,280	1,619	9	4	0	0	0	0	0
52	San Jacinto fault	6.7	923,982	1,321	6	3	0	0	0	0	0
58	Rose Canyon	6.9	923,391	730	3	1	0	0	0	0	0
116	N. C. Pitas Point	6.8	922,902	241	1	0	0	0	0	0	0
69	Coachella valley	7.1	922,793	132	1	0	0	0	0	0	0

Table 2 Results of recorded earthquakes Southern California

Earthquake - Regular So.Cal. database			Network performance [hrs/day]		Bridges status				Link status		
ID	Name	M_w	TTT	Drivers' Delay	min	mod	maj	col	min	mod	maj
34	Northridge (zoom)	6.7	2,339,270	1,416,609	292	197	76	32	47	26	14
23	Northridge	6.7	2,122,280	1,199,619	247	160	57	24	37	21	11
78	Whittier Narrows (zoom)	5.9	1,356,430	433,769	187	113	34	8	31	10	2
56	San Fernando (zoom)	6.7	1,147,040	224,379	132	82	28	11	21	10	4
45	San Fernando	6.7	1,048,550	125,889	92	54	17	6	13	6	2
89	Whittier Narrows	5.9	1,029,270	106,609	116	67	19	6	17	6	1
67	Sierra Madre	5.6	939,427	16,766	40	20	4	1	4	1	0
3	Hwathorne	4.7	934,138	11,477	17	9	2	0	2	0	0
291	Chino Hill	5.4	929,761	7,100	19	10	2	0	2	0	0
777	Beverly Hills	4.2	924,147	1,486	1	0	0	0	0	0	0
784	Beverly Hills	4.2	924,103	1,442	1	0	0	0	0	0	0
399	Whittier Narrows Rec.	4.4	923,497	836	2	1	0	0	0	0	0
12	Landers	7.3	922,807	146	1	0	0	0	0	0	0

Table 3 Results of recorded earthquakes Atlas database

Earthquake – Atlas database			Network performance [hrs/day]		Bridges status				Link status		
ID	Name	M_w	TTT	Drivers' Delay	min	mod	maj	col	min	mod	maj
2032	Northridge	6.7	1,925,300	1,002,639	221	139	47	17	33	17	8
5253	San Fernando	6.6	1,051,390	128,729	95	57	19	7	14	7	3
3115	Whittier Narrows	5.9	948,928	26,267	53	28	7	1	6	2	0
3110	W. N. aftershock	5.2	930,399	7,738	17	8	1	0	1	0	0
2465	Sierra Madre	5.6	925,446	2,785	10	4	0	0	0	0	0
2758	Greater L. A. area	5.7	924,266	1,605	6	3	0	0	0	0	0
2938	Greater L. A. area	5	924,211	1,550	6	3	0	0	0	0	0
3049	Greater L. A. area	4.8	924,191	1,530	6	3	0	0	0	0	0
2031	Greater L. A. area	5.8	923,874	1,213	3	1	0	0	0	0	0
2311	Landers	7.3	923,307	646	3	1	0	0	0	0	0
3460	Central California	6.1	923,000	339	1	0	0	0	0	0	0
5266	Borrego Mountain	6.6	922,970	309	2	1	0	0	0	0	0
5255	Lytle Creek	5.4	922,963	302	2	0	0	0	0	0	0

Table 4 Bridge damage status parameters

| Eq. - Scenario database		Bridges in each damage state							
Name	M_w	min μ	min σ	mod μ	mod σ	maj μ	maj σ	col μ	col σ
San Joaquin Hills	6.6	207.49	12.23	150.48	10.31	68.07	7.83	11.72	3.41
Puente Hills	7.1	602.99	20.15	407.00	17.73	160.83	12.07	66.02	7.85
Chino Hills fault	6.7	103.47	9.38	64.17	7.47	21.30	4.44	3.56	1.88
Newport Ing. fault	6.9	287.67	15.55	183.66	12.29	64.98	7.55	18.57	4.23

Fig. 5 Epicenter of earthquake scenarios
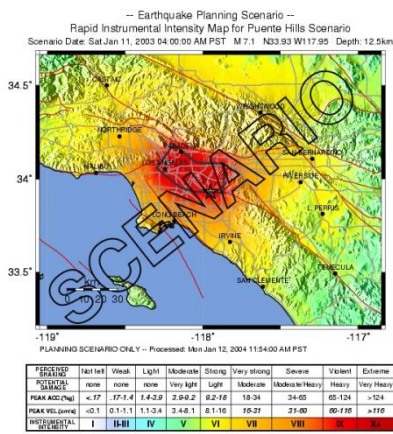
(a) Puente Hills
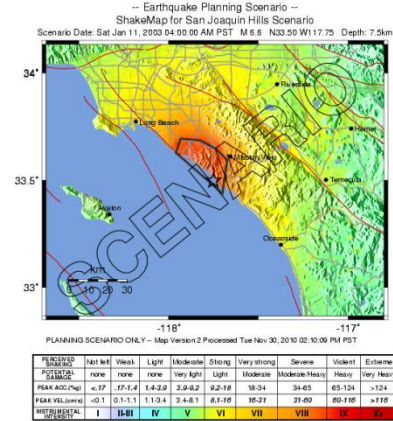
(b) San joaquin Hills
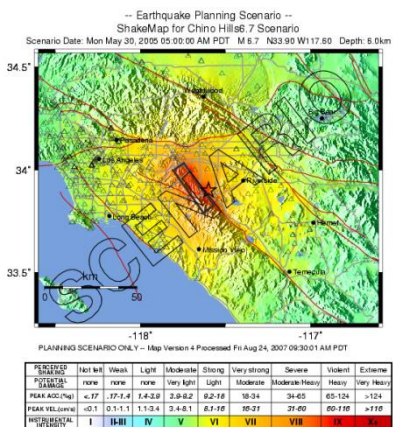
(c) Chino hills
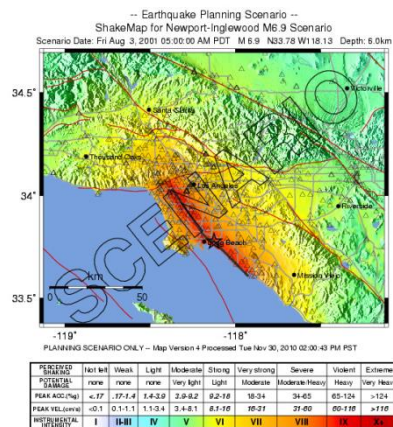
(d) Newport-Inglewood

Fig. 6 Shake map of earthquake scenarios

(a) minor damage

(b) moderate damage

(c) major damage

(d) collapse
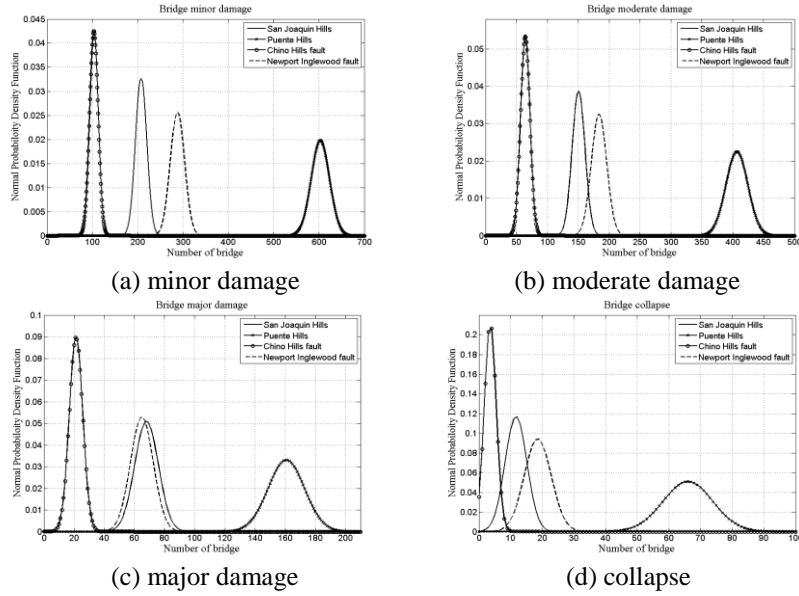
Fig. 7 PDF of bridge damage status

(a) minor damage

(b) moderate damage

(c) major damage

(d) collapse
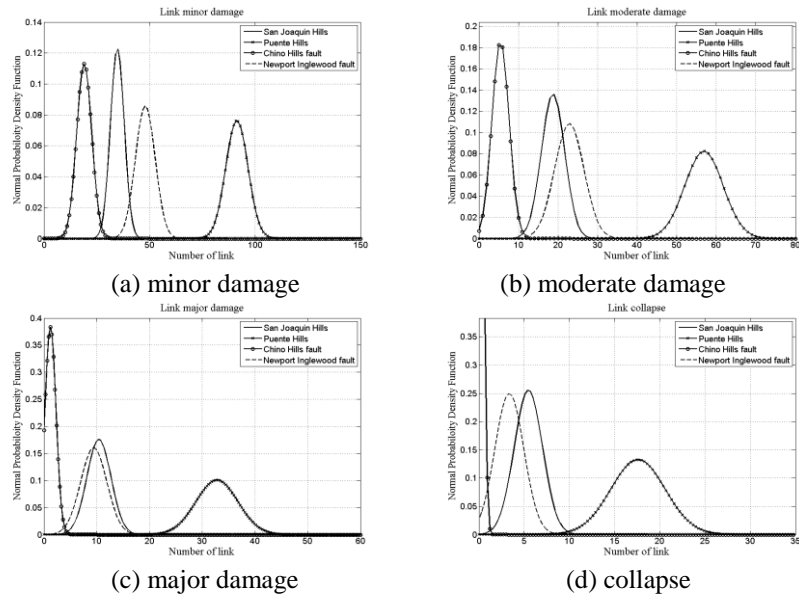
Fig. 8 PDF of link damage status

Table 5 Link damage status parameters

Eq. - Scenario database		Link in each damage state							
Name	M_w	min μ	min σ	mod μ	mod σ	maj μ	maj σ	col μ	col σ
San Joaquin Hills	6.6	34.79	3.25	18.72	2.92	10.42	2.27	5.47	1.56
Puente Hills	7.1	91.46	5.23	56.89	4.85	32.80	3.96	17.59	3.01
Chino Hills fault	6.7	19.09	3.53	5.45	2.14	1.22	1.04	0.13	0.35
Newport Ing. fault	6.9	48.04	4.65	22.83	3.68	9.44	2.49	3.36	1.60

5. Conclusions

The purpose of this study was to develop a framework for the damage assessment of lifeline systems right after an earthquake in quasi-real time. Computer simulations were performed to validate the framework. The simulations were performed for the Los Angeles – Orange County highway transportation network subject to different Shake map. The results express the impact of the earthquake on the network in term of global indexes, such as the social loss due to network disruption, i.e. drivers' delay, and local damage indexes, such as the damage to the bridges and to the links.

The framework has a number of limitations that requires future studies. The hazard is limited by the accuracy of the intensity measure maps. The fragility curves are built based on a prototype, which represents an entire class of bridges with similar characteristics but within the same class differences still exist. Furthermore, throughout the years the structure of the bridges degrades and the fragility curves changes. This non-ergodic behaviour is not considered yet (Der Kiureghian 2005). With an infinite number of Monte Carlo simulations the numerical result always converges to the exact solution but the computational power available limits the accuracy. In this study, computational time is important because the faster the model provides results the sooner the authorities and emergency personnel can use them. 1,000 Monte Carlo simulation were set for the analysis of a scenario because the confidence interval of the mean is less than 3%, which is acceptable. Less than 100 Monte Carlo simulation lead to a confidence interval of the mean as high as 20%. It takes 40 sec to compute and plot the results of a shake map from the moment it is acquired. Intensity measure maps are the current state of art in representing the distribution of an intensity measure of an earthquake over a region of interest and it is made available minutes after the earthquake.

In the future, with tighter networks of strong motion station and more powerful computer the acceleration waveform at any point in the region will be available minutes after the earthquake. This will increase the accuracy of the results in term of both average value and uncertainty.

References

Basoz, N.I., Kiremidjian, A.S., King, S.A. and Law, K.H. (1999), "Statistical analysis of bridge damage data from the 1994 Northridge, CA, earthquake", *Earthq. Spectra*, **15**(1), 25-54.

Der Kiureghian, A. (2005), "Non-ergodicity and PEER's framework formula", *Earthq. Eng. Struct. D.*, **34**(13), 1643-1652.

Fraser, W.A., Wald, D.J. and Lin, K.W. (2008). "Using Shake map and ShakeCast to Prioritize Post-Earthquake Dam Inspections", *Geotechnical Earthquake Engineering and Soil Dynamics Congress IV*.

Karim, K.R. and Yamazaki, F. (2002), "Correlation of JMA instrumental seismic intensity with strong motion parameters", *Earthq. Eng. Struct. D.*, **31**(5), 1191-1212.

Olsen, K.B., Day, S.M., Minster, J.B., Cui, Y., Chourasia, A., Okaya, D., Maechling, P. and Jordan, T. (2008) , "TeraShake2: Spontaneous rupture simulations of M-w 7.7 earthquakes on the southern San Andreas fault", *Bull. Seismol. Soc. Am.*, **98**(3), 1162-1185.

Shin, T., Tsai, Y., Yeh, Y., Liu, C. and Wu, Y. (2002), *Strong-motion instrumentation program in Taiwan*, S. D. Academic, San Diego.

Shinozuka, M., Feng, M.Q., Lee, J. and Naganuma, T. (2000), "Statistical analysis of fragility curves", *J. Eng. Mech. - ASCE*, **126**(12), 1224-1231.

Shinozuka, M., Murachi, Y., Dong, X., Zhou, Y. and Orlikowski, M. (2003), "Effect of seismic retrofit of bridges on transportation networks", *Earthq. Eng. Eng. Vib.*, **2**(2), 169-179.

Shiraki, N., Shinozuka, M., Moore, J.E., Chang, S.E., Kameda, H. and Tanaka, S. (2007), "System risk curves: probabilistic performance scenarios for highway networks subject to earthquake damage", *J. Infrastruct. Syst.*, **13**(1), 43-54.

Torbol, M. and Shinozuka, M. (2012), "Effect of the angle of seismic incidence on the fragility curves of bridges", *Earthq. Eng. Struct. D.*, **41**(14), 2111-2124.

Torbol, M. and Shinozuka, M. (2014), "The directionality effect in the seismic risk assessment of highway networks", *Struct. Infrastruct. E.*, **10**(2), 175-188.

Wald, D., Lin, K.W., Porter, K. and Turner, L. (2008). "ShakeCast: Automating and improving the use of Shake map for post-earthquake decision-making and response", *Earthq. Spectra*, **24**(2), 533-553.

Wald, D. J., Heaton, T., Kanamori, H., Maechling, P.Quitoriano, V. (1996). "Research and development of TriNet 'Shake' Maps", *EOS*, **78**(46), 45.

Wald, D.J., Quitoriano, V., Heaton, T.H. and Kanamori, H. (1999b), "Relationship between peak ground acceleration, peak ground velocity, and modified mercalli intensity for earthquakes in California", *Earthq. Spectra*, **15**(3), 557-564.

Wald, D.J., Quitoriano, V., Heaton, T. H., Kanamori, H., Scrivner, C.W. and Worden, C.B. (1999a). "TriNet 'Shake maps': Rapid Generation of Peak Ground-motion and Intensity Maps for Earthquakes in Southern California", *Earthq. Spectra*, **151**(3), 537-556.

Wald, D.J., Worden, B.C., Quitoriano, V. and Pankow, K.L. (2006), *Shake map® Manual, Technical manual, users guide, and software guide,*, USGS.

Yamakawa, K. (1998), "The prime minister and the earthquake: Emergency management leadership of Prime Minister Marayama on the occasion of the Great Hanshin-Awaji earthquake disaster", *Kansai Univ. Rev. Law and Politics*, **19**, 13-55.

Yamazaki, F., Hamada, T., Motoyama, H. and Yamauchi, H. (1999), "Earthquake damage assessment of expressway bridges in Japan", *Optim.Post-Earthq. Lifeline Syst. Reliab.*, (16), 361-370.

Yamazaki, F., Katayama, T., Noda, S., Yoshikawa, Y. and Ohtani, Y. (1995), *Development of large scale city-gas network alert system based on monitored earthquake ground motion*, JSCE.

CY